The geochemistry of loveringite, a uranium-rare-earth-bearing accessory phase from the Jimberlana Intrusion of Western Australia

I. H. CAMPBELL* AND P. R. KELLY

Department of Geology, School of Earth Sciences, University of Melbourne,
Parkville, Victoria 3052, Australia

SUMMARY. The distribution and geochemistry of lover-ingite, an accessory Ti, Fe $\pm$ Cr oxide containing U and rare-earth elements (Ln) from the Jimberlana Intrusion, have been studied. Loveringite is most abundant in bronzite cumulates; it is found in trace amounts in early plagioclase-augite-hypersthene cumulates, but is not found in the olivine cumulates or in the late-stage differentiates. Loveringites from the bronzite cumulates have a high Cr content compared with those from the plagioclase-augite-hypersthene cumulates, suggesting that the mineral is stabilized by the presence of Cr in the intercumulus liquid. The Ln pattern shows a strong depletion trend from La to Eu, a sharp reversal between Eu and Tb and a second depletion pattern from Tb to Lu. This pattern suggests that the Ln are substituting into two sites, one much larger than the other.

THE rare-earth elements (Ln) belong to the incompatible group of elements, that is, they show little tendency to enter into the structures of common igneous minerals. They concentrate in the residual liquid of a fractionating magma and finally crystallize in certain late-stage accessory minerals. In most igneous rocks the total Ln content of the accessory phases is greater than the Ln content of the primary phases, yet there are few data on the distribution of accessory phases in igneous rocks and only sparse data on Ln patterns in some of these phases. There is a clear need for detailed studies of the distribution and geochemistry of accessory phases in suites of igneous rocks. Such a study has been commenced on the Jimberlana Intrusion of Western Australia and this paper reports on the distribution and geochemistry of loveringite, an accessory Ti, Fe oxide rich in Ln, and other incompatible elements.

Geology of the Jimberlana Intrusion. The Jimber-

lana Intrusion is a layered horizontal pipe-like body (McClay and Campbell, 1976; Campbell, 1977) containing three layered series; the upper layered series (ULS), the lower layered series (LLS), and the marginal layered series (MLS). The LLS consists of a repeated macro-rhythmic succession of olivine and bronzite cumulate layers overlain by a thick layer of plagioclase-augite-hypersthene cumulates. The ULS is similar but has a granophyric layer (55-57 wt. % SiO_2, granophyric texture) at the top of the succession. It is thought to be due to a new pulse of magma that was injected into the magma chamber before crystallization of the LLS had reached the granophyric stage (Campbell, 1977). The MLS is similar to the marginal series of the Muskox Intrusion (Irvine and Smith, 1967).

Most of the samples used in this study come from the LLS, but three samples were included from the granophyric layer of the ULS.

Methods. Loveringite, like many other Ln-bearing accessory phases, occurs in such small quantities that location by microscope techniques is virtually impossible. Fortunately there is a close geochemical link between Ln and U and most, if not all, Ln-bearing accessory phases have a sufficiently anomalous U content to allow them to be located by the fission track method (Kleeman and Lovering, 1967). The technique used in this study was to make a Lexan print of each sample selected for detailed study. All of the U-Ln-bearing accessory phases in the slide (or part of the slide if the number of accessory phases present was large) were then identified using a scanning electron microscope equipped with an energy-dispersive X-ray spectrometer. The nature, size, and abundance of all the U-Ln-bearing accessory phases in each sample were recorded. The method used

* Present address: Department of Geology, University of Toronto, Toronto, Canada M5S 1A1.

is sufficiently reliable to guarantee the location of all U-bearing, and presumably all Ln-bearing, phases in each of the slides examined.

Qualitative electron-probe analyses were carried out on a JEOL electron microprobe using a sample current between 0·2 and 0·4 μA with the beam focused to about 5 μm. Pb, Hf, Zr, Th, Nd, Ce, La, Y, Sr, and V were measured at 20 kV and the remainder at 15 kV. All raw intensity data were corrected by the computer programme of Mason *et al.* (1969). One sample was analysed on an ARL ion microprobe using the procedure described by Lovering (1975).

Distribution. Loveringite occurs as isolated grains that are usually anhedral but occasionally form needles. It is closely associated with other late-stage interstitial minerals especially quartz–K-feldspar intergrowths and phlogopite. The grain-size is normally about 10 × 20 μm but occasional grains up to 120 × 60 μm are found.
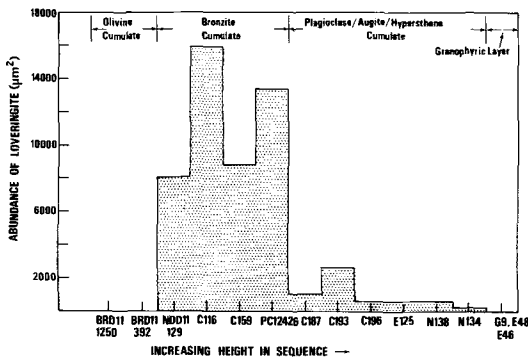

FIG. 1. The approximate amount of loveringite in each sample (as square μm per thin section) estimated from the maximum and minimum dimension of each grain, plotted against height in the sequence. The ultramafic section in the diagram has been simplified to one olivine cumulate layer and one bronzite cumulate layer.

A plot of the amount of loveringite found in each sample against structural height (fig. 1) shows that loveringite is most abundant in the bronzite cumulate layers, occurs in small amounts in the lower half of the plagioclase–augite–hypersthene cumulate layer and is absent from the olivine cumulate layers and the granophyric layer. This distribution pattern suggests that an interaction between pyroxene and the intercumulus liquid may be responsible for the stabilization of loveringite—a point that will be returned to later in the paper.

The amount of loveringite in a rock from a given horizon of the intrusion depends on the degree to which the texture of the rock is orthocumulate. Orthocumulates have more intercumulus liquid and therefore more U, Ln, and other incompatible

elements trapped between the cumulus phases than adcumulates. Consequently, U–Ln-bearing accessory phases are more abundant in orthocumulate rocks than in adcumulate rocks. This point can be illustrated at two levels in the intrusion. First, of the three closely spaced samples from the bottom of the plagioclase–augite–hypersthene cumulate layer (fig. 1), two have an adcumulate texture (C187, C196) and the third (C193) an orthocumulate texture. The orthocumulate has considerably more loveringite than the adcumulates. Secondly, bronzite cumulates from the orthocumulate margin (RRD 4.291) contain more loveringite than stratigraphically equivalent samples from the adcumulate centre (NDD 11.129).

Crystallography. The crystal structure of loveringite has been determined by Gatehouse *et al.* (1978). It is isostructural with senaite, crichtonite, and davidite, having a close-packed anion lattice with a nine-layer (hhc - - -) stacking sequence. Each unit cell contains thirty-nine anion sites of which at least one, the M_0 site, is fully occupied by a large cation. The small cations are distributed over nineteen octahedral and two tetrahedral sites per unit cell (Gatehouse *et al.*, in press). Table I gives a summary of the sites available for cation substitution.

TABLE I. *Summary of cation sites in loveringite*

Site	No.	Size‡	Ions
M_0	1	2·775	Ca, U, Th, Ln (large)
M_1†	1	2·167	Zr, Ln (small), Y, Fe^{2+}, Mn
M_2*	2	1·983	Mg, Fe
M_3†	6	1·975	Fe, Cr, V
M_4†	6	1·972	Ti
M_5†	6	1·971	Ti
—	22		

* Four-fold co-ordination.   † Six-fold co-ordination.   ‡ Metal-oxygen distances.

Geochemistry. Thirty loveringites were analysed by electron microprobe for twenty-one elements and one sample was analysed by ion probe. The ion probe results are given in Table II. Table III gives selected electron microprobe analyses. Loveringite has a very low SiO_2 content, twenty-three of the electron microprobe analyses having less than 0·1 % SiO_2. All analyses which gave over 0·1 % SiO_2 came from small grains (less than 10 × 20 μm), suggesting that the electron beam excited some X-rays from adjacent minerals. These high SiO_2 analyses have been excluded from Table III unless the grain came from a stratigraphic level where no other data were available. The error introduced by

TABLE II. *Ion probe results expressed as atomic %*
or parts per million atomic (ppma) for sample
NDD11.129, grain 18. (Anal. J. F. Lovering.)

Li	0·53 ppma	Fe	1·94%
B	6·99 ppma	Mn	167·14 ppma
F	176·56 ppma	Sr	54·16 ppma
Na	405·66 ppma	Y	51·98 ppma
Mg	1·66%	Zr	0·46%
Al	0·6%	Nb	274·22 ppma
Si	1·89%	Ba	86·34 ppma
P	2·39 ppma	La	172·08 ppma
K	58·65 ppma	Ce	227·55 ppma
Ca	0·65%	Hf	8·8 ppma
Ti	25·64%	Pb	50·0 ppma
V	0·11%	U	16·0 ppma
Cr	1·89%	Th	13·0 ppma

contamination of the spectrum by an adjacent grain is small for most elements but may be significant for Ca, Al, Na, Mg, or K if the adjacent grain is a pyroxene or a feldspar.

Loveringite is a Ti-Fe±Cr oxide, which, by virtue of the six different cation sites available in its structure, may incorporate several other elements in minor quantities. Of these Ca, Zr, Mg, Ln, U, Th, V, and Al are the most important. Gatehouse *et al.* (1978) have demonstrated considerable ordering of the various cations into the different crystallographic sites and the results of their work are summarized in Table I.

There is a stratigraphic control on the Cr content of loveringite. Grains from the bronzite cumulate layers contain 4 to 12% Cr_2O_3, but this falls sharply to less than 0·2% Cr_2O_3 a few metres above the contact with the plagioclase-augite-hypersthene cumulate layer (fig. 2). The drop in the
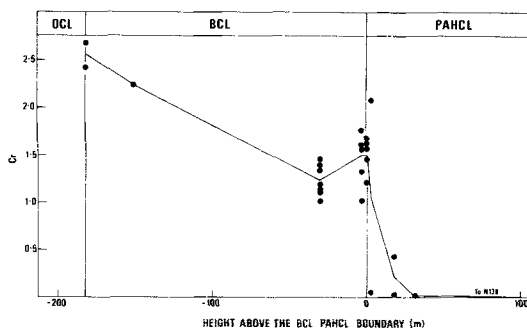

FIG. 2. The Cr content of loveringites, as atoms per thirty-eight oxygens, near the contact between the uppermost bronzite cumulate layer (BCL) and the plagioclase-augite-hypersthene cumulate layer (PAHCL), plotted against height in the sequence. OCL = olivine cumulate layer.

Cr_2O_3 content of loveringite corresponds exactly with the marked decrease in the abundance of the mineral which has already been noted at the same level (fig. 1). Thus the presence of cumulus pyroxene and a high concentration of Cr appear to have an influence on the stability of loveringite.

Careful examination of the bronzite cumulates has revealed a small number of highly resorbed cumulus chromite grains in each sample. Chromite has an incongruent melting relationship (Irvine, 1967; Dickey *et al.*, 1971) with Cr-rich pyroxene and, as Cr is removed from the intercumulus liquid by the crystallization of pyroxene, it is simultaneously replaced by Cr released by the resorption of chromite. Consequently the Cr content of the intercumulus liquid cannot fall below a critical level (i.e. the liquid remains saturated with chromite) as long as some cumulus chromite remains. Thus the loveringites from levels at which chromite is a cumulus phase have a high Cr content because they have crystallized from a chromite-saturated liquid. Once chromite ceased to be a cumulus phase (a little above the bottom of the plagioclase-augite-hypersthene cumulate layer) the high Cr content of the liquid was not maintained during intercumulus crystallization, and there was a dramatic decrease in the abundance and Cr content of the loveringites.

The probable location of Cr^{3+} in the loveringite structure can be demonstrated geochemically. The M_0 and M_1 sites are too large to be suitable for Cr^{3+}. According to crystal-field theory, Cr^{3+} has a strong octahedral site preference and is unlikely to enter the tetrahedral M_2 sites in significant quantities, leaving the M_3, M_4, and M_5 sites as possible locations. Since loveringite may contain up to 12% Cr_2O_3, Cr^{3+} must displace either Fe or Ti from the structure. The M_4 and M_5 sites can be discounted because of their uniform size and scattering characteristics (Gatehouse *et al.*, in press) and because there is no geochemical correlation between Ti and Cr. There is, however, an inverse linear relationship between total Fe and Cr (fig. 3), indicating that Cr is entering the M_3 site, probably at the expense of Fe^{3+}. This conclusion is consistent with the X-ray scattering characteristics of the M_3 site (Gatehouse *et al.*, 1978).

There is also geochemical evidence to support the argument of Gatehouse *et al.* (in press) that most of the large cations are entering the same site (M_0). A plot of Ca against the other large cations shows a strong negative correlation with a slope of 45° (fig. 4).

Ion probe results. The ion probe has detected a number of minor elements including B, F, P, Sr, Nb, Ba, and Hf at the parts per million atomic (ppma) level (Table II). Of particular interest is the very low

TABLE III. *Analyses of loveringites*

	1	2	3	4	5	6	7	8	9	10
TiO_2	59·28	61·56	60·31	56·13	56·14	57·49	59·14	56·82	55·91	56·27
Al_2O_3	0·95	0·95	0·80	0·80	0·91	0·82	1·30	0·63	0·88	0·92
Fe_2O_3	14·21	13·67	21·19	20·52	20·71	20·31	22·89	24·94	19·37	18·49
MnO	0·27	0·28	0·21	0·10	0·14	0·13	0·11	0·10	0·14	0·09
MgO	2·35	2·30	1·52	0·89	0·32	1·25	1·46	0·89	1·23	1·57
CaO	2·54	2·68	2·51	1·67	2·22	2·29	3·23	2·80	1·50	1·80
Cr_2O_3	12·17	11·04	6·48	4·91	7·69	7·37	0·15	1·87	8·21	8·53
SiO_2	—	0·08	—	—	0·02	—	0·93	0·02	0·10	—
Na_2O	0·06	0·05	—	0·02	0·09	0·06	0·15	—	0·04	0·04
K_2O	0·03	0·06	0·06	0·05	0·03	0·05	0·04	0·14	0·03	0·03
NiO	0·04	—	—	0·06	—	—	0·06	0·07	0·08	—
UO_2	—	—	0·09	0·16	0·08	0·17	0·21	0·18	0·17	0·16
PbO	—	—	0·05	—	0·11	0·04	0·09	0·15	—	—
HfO_2	0·27	0·23	0·12	0·31	0·22	0·29	0·21	0·17	0·13	0·18
ZrO_2	5·12	4·43	2·91	4·85	4·69	4·43	5·36	4·96	3·68	4·35
ThO_2	0·13	0·12	0·08	0·19	0·32	0·15	0·41	0·51	0·29	0·51
V_2O_5	0·82	0·70	0·99	1·90	1·41	0·96	0·61	1·03	1·79	1·25
Y_2O_3	0·15	0·11	0·23	0·36	0·23	0·39	0·04	0·09	0·24	0·20
Ce_2O_3	1·38	1·30	1·25	2·79	1·87	1·59	0·20	1·38	2·37	2·54
La_2O_3	1·26	1·23	0·93	1·94	1·02	1·53	0·11	1·20	1·70	2·21
Nd_2O_3	0·23	0·23	0·26	0·43	0·42	0·24	0·01	0·17	0·37	0·38
Ln*	0·55	0·53	0·47	0·97	0·63	0·64	0·06	0·53	0·85	0·98
Sum	101·81	101·55	100·46	99·05	99·27	100·20	96·77	98·65	99·08	100·50

Number of atoms on the basis of thirty-eight oxygens

	1	2	3	4	5	6	7	8	9	10
Ti	12·42	12·83	12·74	12·35	12·23	12·37	12·81	12·45	12·20	12·20
Al	0·31	0·31	0·26	0·28	0·31	0·28	0·44	0·22	0·30	0·31
Fe	2·98	2·85	4·48	4·52	4·51	4·37	4·96	5·47	4·23	4·01
Mn	0·06	0·07	0·05	0·02	0·03	0·03	0·03	0·02	0·03	0·02
Mg	0·98	0·95	0·64	0·39	0·14	0·53	0·63	0·39	0·53	0·67
Ca	0·76	0·80	0·76	0·52	0·69	0·70	0·10	0·87	0·47	0·56
Cr	2·68	2·42	1·44	1·14	1·76	1·67	0·03	0·43	1·88	1·94
Si	—	0·02	—	—	0·01	—	0·27	0·01	0·03	—
Na	0·03	0·03	—	0·01	0·05	0·03	0·08	—	0·02	0·02
K	0·01	0·02	0·02	0·02	0·01	0·02	0·01	0·05	0·01	0·01
Ni	0·01	—	—	0·01	—	—	0·01	0·02	0·02	0·01
U	—	—	0·01	0·01	0·01	0·01	0·01	0·01	0·01	0·01
Pb	—	—	<0·01	—	0·01	<0·01	0·01	0·01	—	—
Hf	0·02	0·02	0·01	0·03	0·02	0·02	0·02	0·01	0·01	0·01
Zr	0·70	0·60	0·40	0·69	0·66	0·62	0·75	0·71	0·52	0·61
Th	0·01	0·01	0·01	0·01	0·02	0·01	0·03	0·03	0·02	0·03
V	0·15	0·13	0·18	0·37	0·27	0·18	0·12	0·20	0·34	0·24
Y	0·02	0·02	0·03	0·06	0·04	0·06	0·01	0·01	0·04	0·03
Ce	0·14	0·13	0·13	0·30	0·20	0·17	0·02	0·15	0·25	0·27
La	0·13	0·13	0·10	0·21	0·11	0·16	0·01	0·13	0·18	0·24
Nd	0·02	0·02	0·03	0·04	0·04	0·02	<0·01	0·02	0·04	0·04
Ln*	0·05	0·05	0·04	0·09	0·06	0·06	0·01	0·05	0·08	0·09
Sum	21·48	21·41	21·34	21·07	21·18	21·32	20·37	21·26	21·21	21·32

* Sum of remaining rare earths calculated from normalized chondrite abundance.

1. NDD11.129, grain B.
2. NDD11.129, grain A.
3. C159, grain 15a.
4. C159, grain 3.
5. PC12.439, grain 11.

6. PC12.426, grain 34.
7. C196, grain 8.
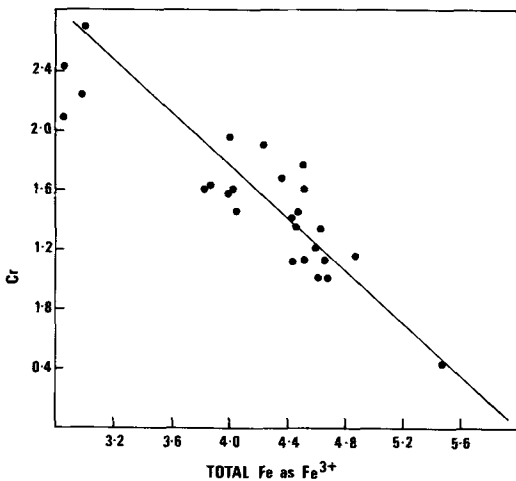8. C193, grain B.
9. RRD4.291, grain 4.
10. RRD4.291, grain 17.

FIG. 3. A plot of Cr against Fe as Fe^{3+}. Both elements are plotted on the basis of atoms per thirty-eight oxygens.
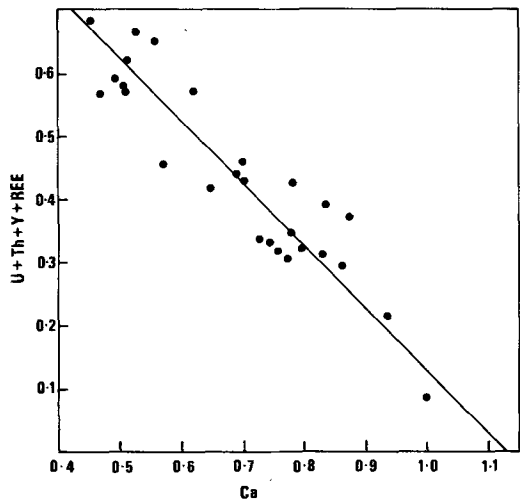

FIG. 4. A plot of Ca against the other large cations (U, Th, Y, and Ln) on the basis of atoms per thirty-eight oxygens.

Sr content of loveringite. The large Sr atom readily enters the M_0 site of the davidite structure and its virtual absence indicates a very low Sr content of the late-stage intercumulus liquid. Another large cation that enters the M_0 site is Pb. The common Pb (204) content of loveringite is below the detection limit of the ion probe, suggesting that the Pb content of the Jimberlana magma was negligible. The Pb detected in loveringite is entirely radiogenic (206, 207, 208) produced by the decay of U and Th. Making the assumption that there is no common lead in Jimberlana loveringites, Wark (*pers. comm.*) has dated the intrusion at 2480 ± 200 Ma from electron microprobe U, Th, and Pb analyses. This date compares favourably with Turek's (1966) Rb–Sr date of 2420 Ma. If loveringite had contained a significant amount of non-radiogenic lead the data obtained by Wark would have been considerably older.

Rare-earth elements. The Ln that were readily detected by electron probe (La, Ce, and Nd) were analysed on a routine basis. The sum of the remaining Ln was calculated by assuming that the ratio of the Ln determined to those not determined was the same as for C193 (Table IV). Two grains

were selected for detailed Ln analyses, one by ion probe (La to Gd only) and the other by electron probe. The results of these analyses are presented in figs. 5 and 6 and Tables IV and V.

Two factors govern the Ln pattern in an accessory mineral: the nature of the sites available in the mineral, and the abundance of each of the Ln in the late-stage intercumulus liquid. The chondrite-normalized Ln pattern for the loveringite grain analysed in detail (fig. 5) shows a depletion in Ln elements from La to Eu, a sharp reversal between Eu and Tb, followed by a second depletion pattern from Tb to Lu. This unusual pattern suggests that the Ln are entering two sites, the M_0 site and the M_1 site. The M_0 site has resulted from the substitution of cations into an anion site (atomic radius of oxygen = 1·40 Å, Shannon and Prewitt, 1969) creating an abnormally large cation site. This site has a preference for cations with an atomic radius considerably larger than La (radius = 1·06 Å), producing the strong depletion pattern from La to Eu. Elements smaller than Eu are too small to enter the M_0 site in significant quantities, but they can substitute for Zr^{4+} and Fe^{2+} in the smaller M_1 site. This site apparently has a prefer-

TABLE IV. *Electron microprobe analyses of Ln in loveringite. Sample C193, grain 2. (Anal. D. Wark.)*

La	Ce	Pr	Nd	Sm	Eu	Gd	Tb	Dy	Ho	Er	Yb
*0·94	1·54	0·16	0·61	0·08	n.d.	0·03	0·05	0·15	0·05	0·03	0·04
†157	100	73	54	22		6	54	24	36	7	10

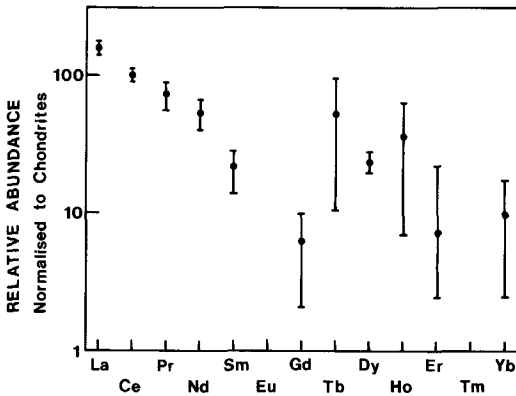* Wt%. † Chondrite normalized and adjusted to Ce = 100.

FIG. 5. Chondrite normalized Ln pattern, adjusted to Ce = 100, for sample C193. Analyst D. Wark, by electron microprobe. Error bars have been calculated from counting statistics ($\pm$ 1o).
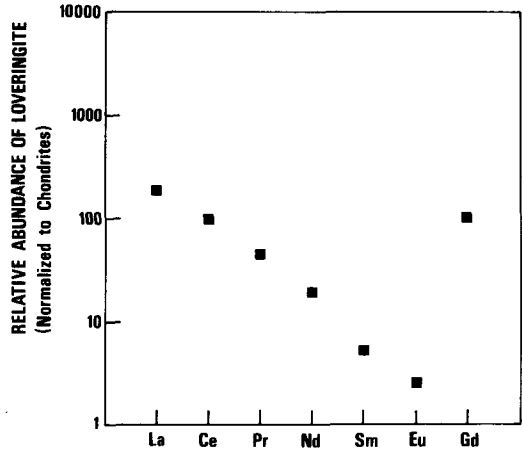

FIG. 6. Chondrite normalized Ln pattern for elements La to Gd adjusted to Ce = 100. Analyst Professor J. F. Lovering, by ion microprobe. Sample NDD11.129, grain 18.

ence for elements with an atomic radius close to 0·90 Å, resulting in a peak near Ho. The exact location of this peak is uncertain due to the errors involved in electron microprobe analyses of Ln elements at low concentrations. The Ln pattern for loveringite is the sum of the M_0 and M_1 patterns. Although the relative abundance of the different Ln in the intercumulus liquid must have played a part in determining the Ln pattern in loveringite, its influence appears to be small as no feature of the loveringite pattern can be attributed to anomalies in the Ln content of the intercumulus liquid.

Davidites have a similar Ln pattern (fig. 7) with the contribution from the smaller Ln centred on Yb, suggesting that the M_1 site may be smaller in davidite than it is in loveringite.

The relationship between loveringite and davidite. The distinction between loveringite and davidite is based on the ratio of the number of Ca:U + Ln in the M_0 site. This ratio must be greater than 1·0 for the mineral to be loveringite (Gatehouse *et al.*, 1978). Ca (r = 1·00 Å) is considerably smaller than La (r = 1·06 Å) and on size criteria is therefore a less favourable cation for entry into the M_0 site. Ca enters the Jimberlana loveringites in appreciable

amounts because its concentration in the Jimberlana magma was several orders of magnitude higher than that of La. Davidite is found in pegmatites and crystallizes from fluids that are high in Ln and low in Ca.

The ratio of Ca:Ln in late-stage intercumulus liquids depends to some extent on the degree to which the texture of the rock is orthocumulate. The more orthocumulate the rock the lower the Ca:Ln ratio and, in extreme orthocumulates, the Ca:Ln

TABLE V. *Ion microprobe analyses of Ln in loveringite. Sample NDD11.129, grain 18, chondrite normalized and adjusted to Ce = 100. (Anal. J. F. Lovering.)*

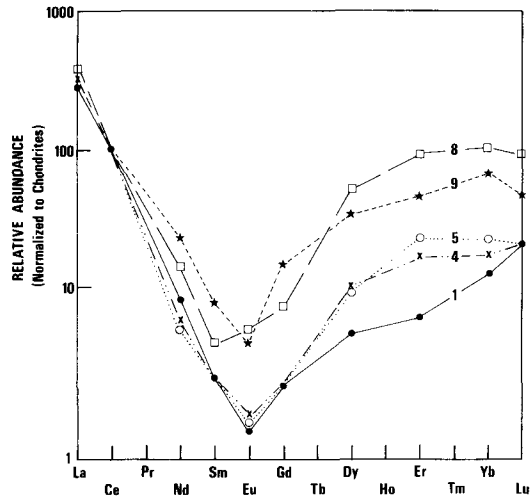| La	Ce	Pr	Nd	Sm	Eu	Gd
188	100	45	19·3	5·2	2·5	102?

FIG. 7. Chondrite normalized Ln pattern for typical davidites adjusted to Ce = 100. Data from Hayton (1960). The numbers refer to Hayton (1960), Table IV. 1 from Tete, Mozambique; 4 and 5 from Radium Hill, South Australia; 8 and 9 from Mount Pleasant, South Australia.

ratio of 'loveringite' may fall below 1·0 (e.g. RRD4.291, grains 4 and 17, Table III). These grains are strictly davidites.

REFERENCES

Campbell (I. H.), 1977. *J. Petrol.* **18**, 183-215.
Dickey (J. S., Jr.), Yoder (H. S., Jr.), and Schairer (J. F.), 1971. *Carnegie Inst. Washington, Yearb.* **70**, 118-22.
Gatehouse (B. M.), Grey (I. E.), Campbell (I. H.), and Kelly (P. R.), 1978. *Am. Mineral.* **63**, 28-36.
Hayton (J. D.), 1960. *Econ. Geol.* **55**, 1030-8.
Irvine (T. N.), 1967. *Can. J. Earth Sci.* **4**, 71-103.
——and Smith (C. R.), 1967. In *Ultramafic and Related Rocks.* Ed. P. J. Wyllie. John Wiley and Sons Inc., New York. Pp. 38-49.
Kleeman (J. D.) and Lovering (J. F.), 1967. *Science,* **156**, 512-13.
Lovering (J. F.), 1975. *N.B.S. Spec. Publ.* **427**.
Mason (P. K.), Frost (M. T.), and Reed (S. J. B.), 1969. *Nat. Phys. Lab. IMS Report I*, 1-91.
McClay (K. R.) and Campbell (I. H.), 1976. *Geol. Mag.* **113**, 129-39.
Shannon (R. D.) and Prewitt (C. T.), 1969. *Acta Crystallogr.* **B25**, 925-46.
Turek (A.), 1966. Ph.D. Thesis, A.N.U., Canberra, Australia.